

Early pattern recognition in severe perinatal asphyxia: a prospective MRI study

O. Baenziger, E. Martin, M. Steinlin, M. Good, R. Largo, R. Burger, S. Fanconi, G. Duc, R. Buchli, H. Rumpel, E. Boltshauser

University Children's Hospital, Zürich, Switzerland

Received: 13 May 1992/Received in revised form: 30 August 1992

Abstract. On the basis of MRI examinations in 88 neonates and infants with perinatal asphyxia, we defined 6 different patterns on T2-weighted images: pattern A – scattered hyperintensity of both hemispheres of the telencephalon with blurred border zones between cortex and white matter, indicating diffuse brain injury; pattern B – parasagittal hyperintensity extending into the corona radiata, corresponding to the watershed zones; pattern C – hyper- and hypointense lesions in thalamus and basal ganglia, which relate to haemorrhagic necrosis or iron deposition in these areas; pattern D – periventricular hyperintensity, mainly along the lateral ventricles, i.e. periventricular leukomalacia (PVL), originating from the matrix zone; pattern E – small multifocal lesions varying from hyper- to hypointense, interpreted as necrosis and haemorrhage; pattern F – periventricular centrifugal hypointense stripes in the centrum semiovale and deep white matter of the frontal and occipital lobes. Contrast was effectively inverted on T1-weighted images. Patterns A, B and C were found in 17%, 25% and 37% of patients, and patterns D, E and F in 19%, 17% and 35%, respectively. In 49 patients a combination of patterns was observed, but 30% of the initial images were normal. At follow-up, persistent abnormalities were seen in all children with patterns A and D, but in only 52% of those with pattern C. Myelination was retarded most often in patients with diffuse brain injury and PVL (patterns A and D).

Key words: Birth asphyxia – Children – Magnetic resonance imaging – Hypoxic ischaemic encephalopathy

Despite major advances in obstetrics and perinatal medicine over the last 20 years the incidence and morbidity of perinatal asphyxia in term infants has changed little [1–4]. Neurological sequelae such as cerebral palsy or devel-

opmental delay occur in 10–25% of affected children [3, 4]. Several retrospective [5–8] and prospective studies [9–12] have tried to establish the predictive value of magnetic resonance imaging (MRI) in children suffering birth asphyxia. Detailed histopathological autopsy studies of hypoxic ischaemic brain injuries have been reported [3, 13, 14], and many workers have described typical signs on ultrasonography and CT [15–17]. Due to limited experience in examining high-risk neonates with MRI, characteristic patterns of cerebral abnormalities following perinatal asphyxia are not well established. The aim of this study was to delineate distinct patterns of pathology in brains of neonates following birth asphyxia, and to look at altered myelination in different areas of the brain, using early MRI examination. Data on neurodevelopmental assessment will be published separately.

Patients and methods

Between 1986 and 1991, 88 neonates, aged 28–42 (mean 38.0) weeks of gestation, who suffered severe perinatal asphyxia were included in a prospective study. Serial MRI examinations were carried out 1–7 days (early MRI), 2–4 weeks (intermediate MRI), and 3, 9 and 18 months after delivery (late MRI). Deviation from this schedule occurred in 12% of patients. The study was approved by the local ethics committee, and informed consent was obtained from the parents. For enrolment into the study three groups of criteria were established (Table 1); at least one item in two groups had to be fulfilled.

Infants with dysmorphic syndromes or malformations, those who required surgery during the neonatal period, and patients with hyaline membrane disease were excluded. The 88 patients finally en-

Table 1. Signs of asphyxia as inclusion criteria

1. Signs of intrauterine asphyxia: bradycardia (heart rate < 80/min), limited beat-to-beat variability, late decelerations, or meconium-stained amniotic fluid
2. Signs of perinatal asphyxia: Apgar score < 5 at 5 min or < 6 at 10 min, umbilical cord artery pH < 7.1, and base deficit < – 10 mmol/l
3. Signs of postpartum encephalopathy during the first 48 h: seizures, lethargy or pathological spontaneous movements

Correspondence to: E. Martin, Division of Magnetic Resonance, Children's University Hospital, Steinwiesstrasse 75, CH-8032 Zürich, Switzerland

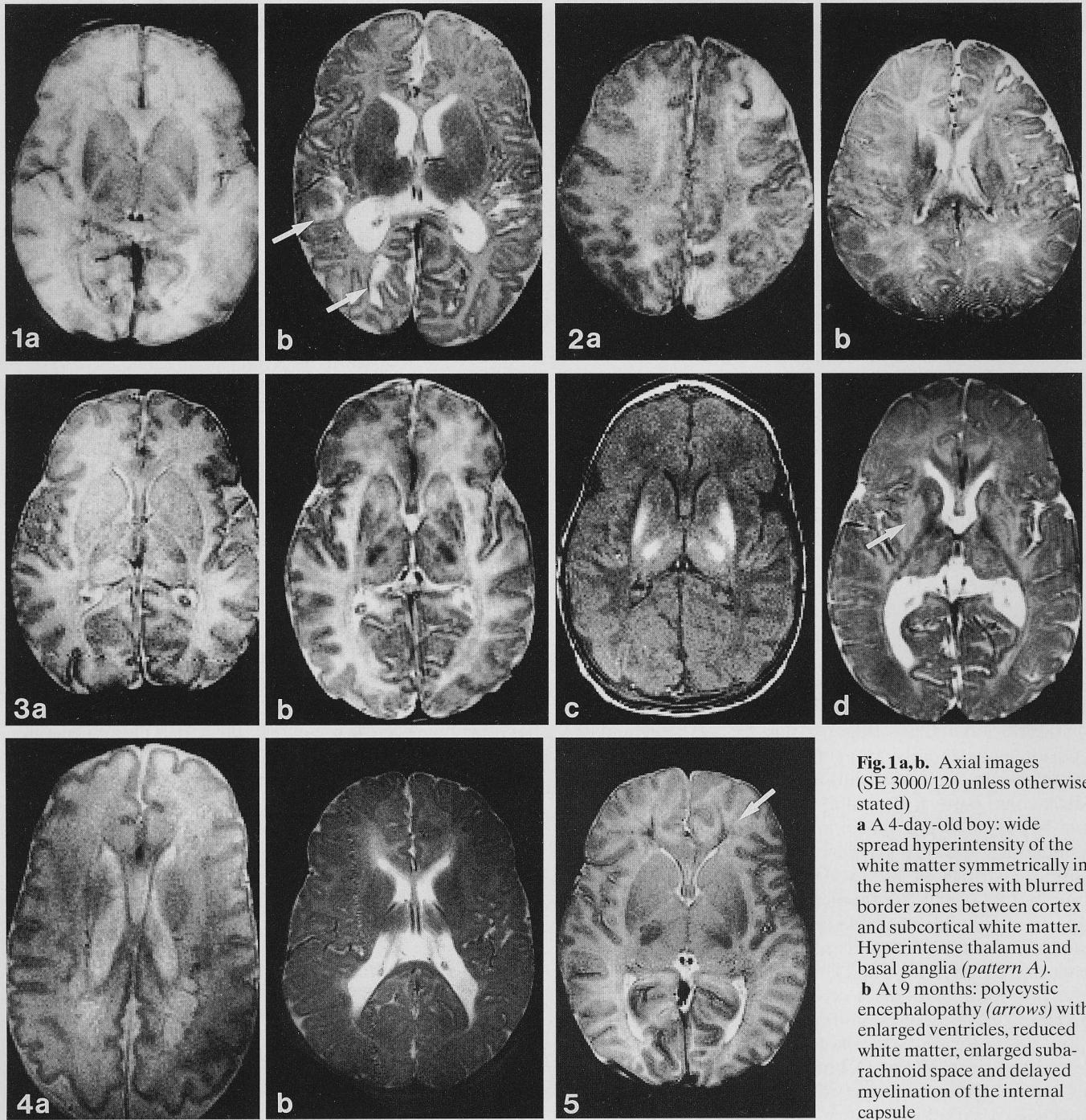


Fig. 2a,b. Axial images. **a** A 6-day-old boy: parasagittal hyperintense lesion in left frontal and occipital lobes with blurred limits between cortex and subcortical white matter. **b** At 9 months: enlarged subarachnoid space, mainly left frontoparietal and reduced white matter bulk in this area

Fig. 3. **a** Axial image. A 2-day-old boy: bilaterally hyperintense basal ganglia and thalamus. **b** At 14 days: bilateral hyperintense regions in the head of the caudate nucleus and anterior internal capsule. The lateral parts of the lentiform nucleus and thalamus are hypointense compared to normal tissue. **c** (SE 500/28). At 14 days: marked bilateral hyperintensity of the lentiform nucleus and thalamus. T1 shortening in the heads of the caudate nuclei (inverse con-

trast to the T2WI). **d** At 9 months: persistent hyperintense changes in thalamus and basal ganglia (*arrow*), asymmetrical enlargement of the lateral ventricles and reduced bulk of occipital white matter

Fig. 4. **a** Axial image. Preterm girl at age 20 days. Multicystic periventricular occipital hyperintensity with partially hypointense border, suggestive of periventricular leukomalacia. **b** At 18 months: enlarged occipital horns, reduced bulk of white matter and delayed myelination

Fig. 5. Axial image. Boy examined on 1st day of life. Thin, periventricular, centrifugal, hypointense stripes extend from the frontal horns (*arrow*) and, less evidently, from the left occipital horn to the periphery of the white matter

Fig. 1a,b. Axial images (SE 3000/120 unless otherwise stated)

a A 4-day-old boy: wide spread hyperintensity of the white matter symmetrically in the hemispheres with blurred border zones between cortex and subcortical white matter. Hyperintense thalamus and basal ganglia (*pattern A*). **b** At 9 months: polycystic encephalopathy (*arrows*) with enlarged ventricles, reduced white matter, enlarged subarachnoid space and delayed myelination of the internal capsule

rolled into the study underwent a total of 196 MRI examinations; each patient underwent 1–5 examinations between the 2nd day and the 6th year of life.

Clinical examination was possible in 56 and 36 children entering the study at the ages of 9 and 18 months, respectively. Four newborns died between 3 and 10 days of age because of postasphyxial encephalopathy and cardiac failure. The parents of 12 infants refused a subsequent MRI examination at 9 months as did those of 15 at 18 months. By January 1992, 14 and 32 patients were younger than 9 and 18 months, respectively, and had not yet been re-examined.

Axial T1-weighted images (T1WI; TR 500 ms, TE 30 ms) and T2-weighted images (T2WI; TR 3000 ms, TE 120 ms) were obtained using a 256 × 256 imaging matrix, on a 2.35 T 40-cm bore system. When parasagittal lesions in very cephalad regions were suspected on axial MRI, additional coronal images were performed. At 3, 9 and 18 months of age the same MRI protocol was used. Myelination was assessed by comparing the MRI pattern of the various brain regions with the normal developmental myelination stages established in earlier studies [19–21].

Results

Postasphyxia patterns on early MRI examinations and their predictive value for late MRI

On the early and intermediate MRI examinations we found six different pathological patterns on T2WI (Table 2).

In *pattern A* there was diffuse hyperintensity of the white matter in both hemispheres, with blurred border zones between cortex and subcortical white matter, indicating diffuse brain injury with cortical necrosis (Fig. 1). Marked hypointensity of the basal ganglia was seen. This pattern was found in both hemispheres of 15 neonates (17%), whose mean gestational age (GA) was 38.2 weeks (32 0/7–39 6/7). The timing of the first MRI and its predictive value (PV) for pathological follow-up MRI are listed

Table 2. MRI patterns in neonatal brain following perinatal asphyxia (T2-weighted images)

Pattern A:	Diffuse hyperintensity of cerebral hemispheres
Pattern B:	Hyperintensity of parasagittal watershed regions
Pattern C:	Lesions in basal ganglia or thalamus
Pattern D:	Periventricular hyperintensity
Pattern E:	Focal parenchymal ischaemia or haemorrhage
Pattern F:	Periventricular centrifugal hypointense stripes
Pattern G:	Normal

in Table 3. All 15 children showed typical postasphyxial abnormalities on late MRI (PV = 100).

Pattern B showed parasagittal hyperintensity, mainly in the centrum semiovale, but involving the cortex, seen on coronal sections to correspond to the mature boundary zone between the anterior and middle, and middle and posterior cerebral arteries respectively. There were 22 patients (25%), 39.2 weeks GA (range 38 2/7–40 6/7), who showed this pattern, with unilateral or bilateral lesions (Fig. 2). In 3 of 4 patients small, isolated watershed lesions on early MRI unexpectedly resolved on subsequent examinations. All were initially detected between day 1 and day 7. The PV of the early MRI in group B was 50% (Table 3).

Pattern C consisted of lesions in the thalamus and/or basal ganglia, and was observed in 33 infants (37%), mean GA 37.8 weeks (range 28 0/7–42 2/7). The pathological findings were predominantly in the lateral putamen and showed a mixed hypo- and hyperintense pattern, reversed on T1WI (Fig. 3). The PV of the early MRI was 66 (6 of 9), while 9 of 19 patients with positive findings on intermediate MRI demonstrated persistent changes on the late study (PV = 47.5) (Table 3). Three patients with an isolated defect in the thalamus or basal ganglia on early MRI had a normal thalamus or basal ganglia at follow-up (Table 3). The neurodevelopmental outcome of all these children was poor [18].

In *pattern D*, periventricular hyperintensities (PVH) were located mainly posterior and lateral to the occipital horn, anteriorly to the frontal horn or in the corona radiata in 17 children (19%), mean GA 37.0 weeks (range 31 0/7–40 1/7) (Fig. 4). The mean GA was significantly lower ($P < 0.05$) than that in children showing patterns A, B, C or F. The lesions represented oedema or necrosis – periventricular leukomalacia (PVL), leading eventually to gliosis or to cystic formation. Nine of 12 patients showed marked enlargement of the ventricles and atrophy of white matter at 3 and 9 months (Table 3). All 3 patients with isolated PVL had reduced white matter mass and marked enlargement of the ventricles at follow-up.

Pattern E included multiple small white matter lesions of varying in contrast from hyperintense to hypointense, interpreted on the early MRI as necrosis in 9 patients and haemorrhages in 6. Three of the 9 patients with focal necrosis had lesions the territory of the middle cerebral artery; the remainder were in different areas.

Table 3. Predictive value of pathological patterns on early and intermediate MRI in relation to follow-up

Pattern	MRI pattern											
	A		B		C		D		E		G	
Time of MRI (days)	0–7	14–28	0–7	14–28	0–7	14–28	0–7	14–28	0–7	14–28	0–7	14–28
Number	8	7	13	9	13	20	11	6	7	8	12	14
Death	4				2				2			
Follow-up examinations	4	5	10	8	9	19	7	5	4	7	10	10
Persistent lesions	4	5	5	4	6	9	5	4	4	7	1	0
Predictive value (%)	100	100	50	50	66	47.5	66	75	100	100	90	100

Table 4. Combinations of MRI patterns

Associated pattern	Principal pattern					
	A ^a	B	C	D	E	F
Number	15	22	33	17	15	31
None	0	4	4	3	3	0
A	—	—	10 (30)	—	1 (7)	1 (3)
B	—	—	10 (30)	3 (17)	3 (20)	4 (13)
C	10 (66)	10 (45)	—	9 (53)	5 (33)	16 (52)
D	—	3 (13)	9 (27)	—	5 (33)	10 (32)
E	1 (7)	3 (13)	5 (15)	5 (30)	—	7 (23)
F	5 (33)	3 (13)	16 (48)	10 (60)	7 (47)	—

Percentage is given in parenthesis

^a Pattern A excludes combination with B or D by definition. The principal pattern may be combined with more than one additional pattern

^b Percentages in parentheses

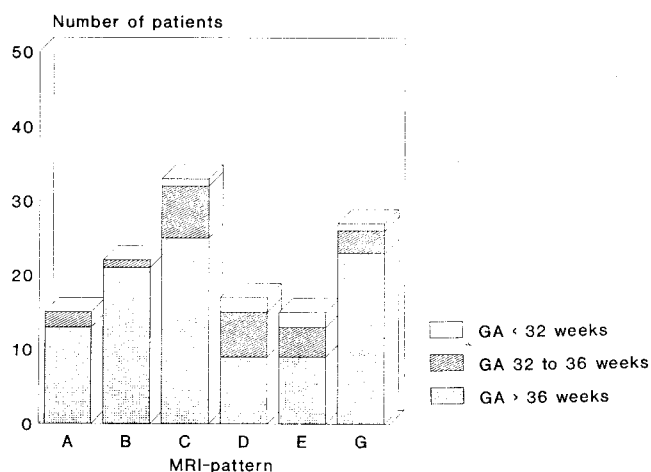


Fig. 6. Number of premature and term neonates with MRI patterns A–E and G

The mean GA of group E was 36.5 weeks (range 28 0/7–38 2/7).

The main features of *pattern F* were thin, centrifugal, periventricular hypointense stripes predominantly in the centrum semiovale and the frontal and occipital lobes. These stripes could be delineated in 31 patients (35%), whose mean GA was 38.2 weeks (range 34 0/7–40 1/7). Although clearly seen on and MRI studies within 20 days of birth, they were never present on later examinations. This pattern was always seen in combination with one or other of patterns A–E, never as an isolated finding (Fig. 5).

Patterns A–F occurred isolated or in mutual combinations (Table 4).

Pattern G involved normal MRI findings. In 26 of 88 (30%) asphyxiated newborns early MRI was normal, but on follow-up 4 of 20 had PVH, and 3 showed mild occipital horn dilatation on late MRI (PV = 35). None of these patients showed severe brain atrophy or delayed myelination (PV = 100).

Figure 6 shows the number of preterm and term neonates with patterns A–E and G. Partial necrosis of the left cerebellar hemisphere and a small cerebellar haemorrhage were found in 2 term infants with prolonged severe asphyxia.

Stage of myelination at follow-up in relation to patterns A–E on early/intermediate MRI

Transient or permanent delayed myelination in various areas of the brain, the telencephalon, basal ganglia, internal capsule, corpus callosum, the posterior visual pathways, descending tracts, the midbrain, pons, or the cerebellum was seen in 39 of 56 children (70%).

None of the 15 infants with *pattern A* had a normal myelination of the telencephalon. Seven showed delayed or defective myelination of the basal ganglia or thalamus. Altered myelination was found in the internal capsule in 9 infants, in the corpus callosum in 9, in the posterior visual pathway in 6, and in the descending tracts of the pons and medulla in 3.

Of the 22 infants with *pattern B*, 18 were re-examined, 4 being lost to follow-up; 12 had pathological myelination of the telencephalon. Nine had frontal and/or occipital periventricular, hyperintense, round foci (PVH grade I [22]). Three of 4 patients with isolated parasagittal changes on early MRI had normal myelination, and 1 showed PVH.

Of the 33 patients with *pattern C*, 28 were re-examined; 3 died within a few days and 1 was lost to follow-up. Pathological myelination of the basal ganglia or thalamus was seen in 13.

We followed 12 of the 22 children with *pattern D* for more than 3 months: 8 had pathological periventricular myelination, and 6 slightly delayed myelination of the telencephalon. Of 3 patients with isolated PVH 1 demonstrated delayed myelination of the whole telencephalon, the internal capsule on one side and the basal ganglia.

PVH was detected at 3 months in 24 patients, and persisted on later follow-up in 22. Its extent of PVH varied: it was grade I (round foci adjacent to the frontal or occipital horns on T2WI) in 19 patients and grade II (along the whole lateral ventricle) [22] in 4. Only 8 (33%) of these children had evidence of PVH on the early MRI.

In the 3 patients with *pattern E*, with focal lesions and no other abnormality, myelination was otherwise normal.

In 20 infants with no pathological findings on early MRI, 4 showed grade I PVH.

Discussion

Abnormal MRI patterns were found in 70% of the initial examinations, and were probably related to hypoxic ischaemic brain injury. The higher rate of positive findings than in other studies [11] may be due to our definition of asphyxia and strict inclusion criteria (Table 1); 82 of the 88 neonates had to be ventilated initially.

Pattern A diffuse hyperintensity of the cerebral hemispheres was seen predominantly in full-term neonates. Because of the high water content in the brain of preterm infants diffuse injury can be detected more readily in more mature infants [5]. In accordance with our previous study [12] a thin hyperintense cortex was found on T1WI in this group. At follow-up all these infants showed marked abnormalities, with multicystic leukomalacia, enlargement

of the ventricles or cerebral atrophy, as a consequence of reduced bulk of white matter and delayed myelination.

In children with hyperintensity of the parasagittal watershed regions (*pattern B*), only 50% of lesions identified on early and intermediate MRI could be confirmed at follow-up (PV = 50). We believe that the localized hyperintensity might often be due to oedema, which subsequently resolves.

Involvement of the thalamus and basal ganglia (*pattern C*) is infrequently described neuropathologically [23–25], although there are recent case reports of ultrasound, CT and MRI [26–28]. In the present study 33 of 88 children had these lesions. They may be due to necrosis or be produced by iron deposits from small haemorrhages or iron-containing enzymes within the basal ganglia and thalamus. Furthermore, iron transportation is defective in damaged neurons and the metal accumulates in the proximal axon of injured neurons [29]. The high magnetic field (2.35 T) renders the system very sensitive to changes in magnetic susceptibility.

PVL is the most frequently described nonhaemorrhagic brain lesion in preterm infants [30, 31]. Our patients with PVH (*pattern D*) on early MRI had a significantly lower GA than those with other brain lesions. Due to the under-representation of very low birthweight preterm infants in this study (Fig. 6), there were only 17 children with periventricular lesions. In images of very premature babies differentiation of PVL from normal brain is difficult due to the higher water content of the brain [5]. The PVL were mainly adjacent and later to the occipital horn, anterior to the frontal horn or in the corona radiata. At 3 months of age ventricular enlargement was found which remained constant during the first 18 months in 75% of our patients with PVH. Of the 24 patients with PVH at the age of 3 months or more, only 8 (33%) had signs of PVL on early MRI. This illustrates, in contrast to the findings of other authors [6, 8], that PVH is seen on late MRI not only in infants with known PVL, but also often in other children with severe perinatal asphyxia [22]. The pathophysiological substrate of PVH is probably an increased water content of the periventricular tissue. This may result from delayed production or destruction of hydrophobic myelin, periventricular oedema, or gliosis following neuronal death. Other workers, grading PVH in three or five stages, found a good correlation between the extent of PVH and clinical outcome [22, 32]. Round foci adjacent to the frontal and occipital horns are very frequent and seem to be consistent with normal or near normal brain development [22, 31, 32].

The hypointense centrifugal stripes (*pattern F*), described first in an earlier study [12], are always associated with other white matter lesions. The aetiology and significance of these stripes remain uncertain. We speculate that enlargement of vessels during the postasphyxial loss of autoregulation, or capillary bleeding could be responsible.

Myelination was predominantly delayed on follow-up examinations with patterns A and D. In pattern E, i.e. focal parenchymal ischaemia or haemorrhage, the delay in myelination depended on the location and extent of the hypoxic defect and on the number of associated lesions.

The stage of myelination on the early MRI is not as useful a marker of perinatal hypoxic-ischaemic encephalopathy as it is in later images [7].

Acknowledgement. This work was supported by the Swiss National Foundation, grant no. 32-30176.90

References

- Robertson C, Finner N (1985) Term infants with hypoxic-ischemic encephalopathy: outcome at 3.5 years. *Dev Med Child Neurol* 27: 473–484
- Volpe JJ (ed) (1987) *Neurology of the newborn*. Saunders, Philadelphia, pp 258–262
- Levene M (ed) (1987) *Neonatal neurology*. Churchill Livingstone, Edinburgh, pp 157–200
- Nelson KB, Leviton A (1991) How much of neonatal encephalopathy is due to birth asphyxia? *Am J Dis Child* 145: 1325–1331
- McArdle CB, Richardson CJ, Hyden CK, Nicholas DA, Amparo EG (1987) Abnormalities of the neonatal brain: MR imaging. II. Hypoxic-ischemic brain injury. *Radiology* 163: 395–403
- Barkovich AJ, Truwit CL (1990) Brain damage from perinatal asphyxia: correlation of MR findings with gestational age. *AJNR* 11: 1087–1096
- Byrne P, Welch R, Johnson MA, Darrah J, Piper M (1990) Serial magnetic resonance imaging in neonatal hypoxic ischemic encephalopathy. *J Pediatr* 117: 694–700
- Truwit CL, Barkovich AJ, Koch TK, Ferriero DM (1992) Cerebral palsy: MR findings in 40 patients. *AJNR* 13: 67–78
- Johnson MA, Pennock JM, Bydder GM, Dubowitz LMS, Thomas DJ, Young IR (1987) Serial MR imaging in neonatal cerebral injury. *AJNR* 8: 83–92
- Keeney SE, Adcock EW, McArdle CB (1991) Prospective observations of 100 high-risk neonates by high-field (1.5 Tesla) magnetic resonance imaging of the central nervous system. I. Intraventricular and extracerebral lesions. *Pediatrics* 87: 421–430
- Keeney SE, Adcock EW, McArdle CB (1991) Prospective observations of 100 high-risk neonates by high-field (1.5 tesla) magnetic resonance imaging of the central nervous system. II. Lesions associated with hypoxic-ischemic encephalopathy. *Pediatrics* 87: 431–438
- Steinlin M, Dirr R, Martin E, Boesch C, Largo RH, Fanconi S, Boltshauser E (1991) MRI following severe perinatal asphyxia: preliminary experience. *Pediatr Neurol* 7: 164–170
- Larroche JC (1977) *Developmental pathology in neonates*. Excerpta Medica, Amsterdam
- Leech R, Alvord EC (1977) Anoxic-ischemic encephalopathy in the human neonatal period. The significance of brainstem involvement. *Arch Neurol* 34: 109–113
- Flodmark O, Fitz CR, Harwood-Nash DC (1980) Computed tomographic diagnosis and short-term prognosis of intracranial hemorrhage and hypoxic-ischemic brain damage in neonates. *J Comput Assist Tomogr* 4: 775–787
- Lipp-Zwahlen AE, Deonna T, Micheli JL, Calame A, Chrzanowski R, Cetre E (1985) Prognostic value of neonatal CT scans in asphyxiated term babies: low density score compared with neonatal neurological signs. *Neuropediatrics* 16: 209–217
- Dubowitz LMS, Bydder GM, Mushin J (1985) Developmental sequence of periventricular leukomalacia. Correlation of ultrasound, clinical and magnetic resonance functions. *Arch Dis Child* 60: 349–355
- Deleted
- Martin E, Boesch C, Zuerrer M, Kikinis R, Molinari L, Kaelin P, Boltshauser E, Duc G (1990) MR imaging of brain maturation in normal and developmentally handicapped children. *J Comp Assist Tomogr* 14: 685–692

20. Stricker T, Martin E, Boesch C (1990) Development of the human cerebellum observed with high-field-strength MR imaging. *Radiology* 177: 431–435
21. Martin E, Krassnitzer S, Kaelin P, Boesch C (1991) MR imaging of the brainstem: normal postnatal development. *Neuroradiology* 33: 391–395
22. Konishi Y, Kuriyama M, Hayakawa K, Konishi K, Yasujima M, Fujii Y, Sudo M (1990) Periventricular hyperintensity detected by magnetic resonance imaging in infancy. *Pediatr Neurol* 6: 229–232
23. Rosales RK, Riggs HE (1962) Symmetrical thalamic degeneration in infants. *J Neuropathol Exp Neurol* 21: 372–376
24. Norman MG (1972) Antenatal neuronal loss and gliosis of the reticular formation, thalamus, and hypothalamus. *Neurology* 22: 910–916
25. Myers RE (1975) Four patterns of perinatal brain damage and their conditions of occurrence in primates. In: Meldrum BS, Marsden CD (eds) *Advances in neurology*. Raven Press, New York, pp 223–234
26. DiMario FJ, Clancy R (1989) Symmetrical thalamic degeneration with calcification of infancy. *Am J Dis Child*
27. Voit T, Lemburg P, Neuen E, Lumenta C, Stork W (1987) Damage of thalamus and basal ganglia in asphyxiated full-term neonates. *Neuropediatrics* 18: 176–181
28. Eicke M, Briner J, Willi U, Uehlinger J, Boltshauser E (1992) Symmetrical thalamic lesion in infants. *Arch Dis Child* 67: 15–19
29. Dietrich RB, Bradley WG (1988) Iron accumulation in the basal ganglia following severe ischemic anoxic insults in children. *Radiology* 168: 203–206
30. Wilson DA, Steiner RE (1986) Periventricular leukomalacia: evaluation with MR imaging. *Radiology* 160: 507–511
31. Flodmark O, Lupton B, Li D (1989) MR imaging of periventricular leukomalacia in childhood. *AJR* 152: 583–590
32. Zimmermann RD, Flemming CA, Lee BCP, Saint-Louis LA, Deck MD (1986) Periventricular hyperintensity as seen by magnetic resonance: prevalence and significance. *AJNR* 7: 13–20